Cell Stress and Chaperones (2023) 28:861–876
https://doi.org/10.1007/s12192-023-01380-7

ORIGINAL ARTICLE

RBM25 regulates hypoxic cardiomyocyte apoptosis through CHOP-associated endoplasmic reticulum stress

Ziwei Zhu[1] · Jie Pu[1] · Yongnan Li[2] · Jianshu Chen[1] · Hong Ding[1] · Anyu Zhou[3] · XiaoWei Zhang[1]

Received: 30 May 2023 / Revised: 15 August 2023 / Accepted: 10 September 2023 / Published online: 22 September 2023
© The Author(s), under exclusive licence to Cell Stress Society International 2023

Abstract

Ischemic heart failure (HF) is one of the leading causes of global morbidity and mortality; blocking the apoptotic cascade could help improve adverse outcomes of it. RNA-binding motif protein 25 (RBM25) is an RNA-binding protein related to apoptosis; however, its role remains unknown in ischemic HF. The main purpose of this study is to explore the mechanism of RBM25 in ischemic HF. Establishing an ischemic HF model and oxygen-glucose deprivation (OGD) model. ELISA was performed to evaluate the BNP level in the ischemic HF model. Echocardiography and histological analysis were performed to assess cardiac function and infarct size. Proteins were quantitatively and locationally analyzed by western blotting and immunofluorescence. The morphological changes of endoplasmic reticulum (ER) were observed with ER-tracker. Cardiac function and myocardial injury were observed in ischemic HF rats. RBM25 was elevated in cardiomyocytes of hypoxia injury hearts and localized in nucleus both in vitro and in vivo. In addition, cell apoptosis was significantly increased when over-expressed RBM25. Moreover, ER stress stimulated upregulation of RBM25 and promoted cell apoptosis through the CHOP related pathway. Finally, inhibiting the expression of RBM25 could ameliorate the apoptosis and improve cardiac function through blocking the activation of CHOP signaling pathway. RBM25 is significantly upregulated in ischemic HF rat heart and OGD model, which leads to apoptosis by modulating the ER stress through CHOP pathway. Knockdown of RBM25 could reverse apoptosis-mediated cardiac dysfunction. RBM25 may be a promising target for the treatment of ischemic HF.

Keywords Ischemic heart failure · Myocardial infarction · Apoptosis · Endoplasmic reticulum stress · RBM25

Abbreviations

ARGs	Apoptosis-related genes
BBC3	BCL2-binding component 3
CHOP	C/EBP homologous protein
DEGs	Differentially expressed genes
EF	Ejection fraction
ER	Endoplasmic reticulum
FS	Fractional shortening
GO	Gene Ontology
GFP	Green fluorescent protein
H&E	Hematoxylin-eosin
KEGG	Kyoto Encyclopedia of Genes and Genomes
LVEDD	Left ventricular end-diastolic inner diameter
LVEDV	Left ventricular end-diastolic volume
LVESD	Left ventricular end-systolic inner diameter
LVESV	Left ventricular end-systolic volume
MI	Myocardial infarction
OGD	Oxygen-glucose deprivation
RBM25	RNA-binding motif protein 25
SD	Sprague-Dawley
UPR	Unfolded protein response

Introduction

Ischemic heart failure (HF) is an important cause of high morbidity and mortality worldwide, resulting in an increasing health and economic burden (Heidenreich et al. 2022). There are approximately 64 million people with HF worldwide, and the prevalence of HF is on the rise due to an aging population, an increasing burden of HF comorbidities and risk factors, and longer survival after myocardial infarction (MI) (Castiglione et al. 2022).

✉ XiaoWei Zhang
xwzhang@lzu.edu.cn

[1] Department of Cardiovascular Medicine, Lanzhou University Second Hospital, Lanzhou 730000, China

[2] Department of Cardiac Surgery, Lanzhou University Second Hospital, Lanzhou 730000, China

[3] Department of Cardiology, Warren Alpert School of Medicine at Brown University, Providence, RI, USA

Apoptosis is an important pathological mechanism in the development of HF, and the intervention of the cascade reaction process of apoptosis can improve the adverse outcomes of HF (Gustafsson and Gottlieb 2003). Accumulating evidence indicates that apoptosis induced by endoplasmic reticulum (ER) stress is often associated with cardiac structural or functional abnormalities in HF patient [4; 5].

The pathological process of HF is accompanied by disruption of protein homeostasis, leading to the accumulation of unfolded or misfolded proteins in the ER. Central to the regulation of protein homeostasis in the ER is the unfolded protein response (UPR), a signaling pathway that regulates cellular protein folding capacity to maintain cellular secretory function. Maladaptive or terminal UPR occurs when the adaptive UPR fails to maintain ER homeostasis, leading to disruption of ER integrity and apoptosis (Ren et al. 2021). ER stress induces apoptosis mainly through the IRE1/ASK1/JNK pathway, the caspase-12 kinase pathway, and the C/EBP homologous protein (CHOP)/GADD153 pathway (Hu et al. 2018). CHOP, also known as DNA damage-inducible transcript 3, is considered a specific and convergent transcription factor of ER stress, and its expression is often regulated at the transcriptional level (Yang et al. 2017). Apoptosis is the main cellular function of CHOP. Under the stimulation of pathological injury factors, ER stress increases the expression of CHOP and activates apoptosis (Yao et al. 2017).Based on the above, CHOP has gradually become the focus of ER stress researches.

RNA-binding motif protein 25 (RBM25) is an RNA-binding protein (Carlson et al. 2017). Although it has been demonstrated that RBM25 is increased in human HF cardiac tissue samples (Gao et al. 2011), and RBM25 has been found to be closely related to apoptosis, the specific molecular mechanism leading to cell apoptosis remains unclear. A large number of studies have shown that ER stress-induced apoptosis in HF exacerbates the progression of HF [6; 12; 13], but the mechanism of RBM25 regulating ER stress-mediated apoptosis in HF has not been reported. Therefore, our research aims to clarify the molecular mechanism of RBM25 regulating ER stress-mediated apoptosis in HF, to add new theoretical knowledge to the molecular mechanism of HF and provide potential new therapeutic strategies for HF.

Materials and methods

Animals

All animal procedures were approved by the Ethics Committee of Lanzhou Second Hospital, Lanzhou University(D2022-444) and were performed according to the guidelines of the National Institutes of Health Guidelines for the Care and Use of Laboratory Animals.

All Sprague-Dawley (SD) (body weight 200–240 g, male) rats and C57BL/6 N (body weight 22–26 g, male) mice were kept at a constant temperature (21–24°C) and were given free access to water and standard chow diet. The establishment of the rat and mice MI (ischemic HF) model was performed. The rats were anesthetized with 3% sevoflurane and fixed on a hardboard for preoperative left chest skin preparation. The tracheal cannula was inserted through the mouth of rats and attached to a small animal ventilator. The left anterior descending coronary artery was ligated at the level between the pulmonary artery cone and the left atrial appendage. It can be observed that the color changes from red to white from the ligation site to the apex of the heart. The chest was then closed, the incision disinfected with iodophor, and 100,000 units of penicillin was administered intravenously to prevent infection. Sham-operated rat underwent the same procedure without coronary artery ligation. Rats were randomly assigned into 5 groups: Sham group, MI-1 W group, MI-2 W group, MI-3 W group, and MI-4 W group.

The mice MI model was established by ligating the left anterior descending branch of the coronary artery. After simple anesthesia, blunt incision was made at the intersection of the left midclavicular line and the left margin of the sternum between the 3rd and 4th ribs. The ribs were excised, and the chest was opened. The pericardium was then separated with hemostatic forceps. Simultaneously, the heart was squeezed upwards with the thumb and index finger, with the sternum flipped slightly to find the LAD artery, which was ligated with the 6-0 silk thread at the left atrial appendage 1–2 mm below the pulmonary artery cone junction. The mice were randomly divided into three groups: MI alone (MI) group, an empty vector adenovirus (MI + shCON) group, and an RBM25 knockdown (MI + shRBM25) group. Modeling mice in MI + shCON and MI + shRBM25 groups were injected with adeno-associated virus 9 (AAV9) via caudal vein, while mice in MI group were injected with 0.9% normal saline solution. AAV9 (Shanghai Jikai Biotechnology Co., Ltd., Shanghai, China) was used for the specific knockdown of RBM25.

Echocardiography

Transthoracic echocardiographic measurements were performed on all rats/mice using a Philips instrument (EPIQ 7, Royal Philips of the Netherlands Inc. Amsterdam, Netherlands) equipped with a 22 MHz phased array linear transducer (el18-4, Royal Philips of the Netherlands Inc. Amsterdam, the Netherlands) for continuous assessment of

cardiac structure and function. Ejection fraction (EF), left ventricular fractional shortening (FS), the left ventricular end-diastolic inner diameter (LVEDD), left ventricular end-diastolic volume (LVEDV), left ventricular end-systolic inner diameter (LVESD), and left ventricular end-systolic volume (LVESV) were obtained and calculated.

Histopathology evaluation

Heart tissue samples were taken and stained with hematoxylin-eosin (H&E) and Masson according to manufacturer's instructions. For the Masson staining, the number of cardiac constrictor zone necrosis was counted using ImageJ 8.4 software (National Institutes of Health, USA).

Immunofluorescence staining

The sections/AC16 were incubated with 0.5% Triton X-100 for 30 min and then blocked with bovine serum albumin. Slices were then incubated overnight with primary antibody at 4 °C and then with secondary antibody conjugated with Alexa Fluor 488 or Alexa Fluor 647. Finally, the nuclei were stained with 4′,6-diamidino-2-phenylindole (DAPI, Sigma-Aldrich) for 20 min at room temperature before observation under a confocal microscope (Carl Zeiss, Oberkochen, Germany). The antibodies used in this study were RBM25 (1:200, Abcam, Cambridge, UK) and cardiac troponin I (1:200, Proteintech, Wuhan, China).

Enzyme-linked immunosorbent assay (ELISA)

The contents of BNP in serum were detected using ELISA kits (Baizhou, Shanghai, China) according to the manufacturer's instructions.

Electron microscopy

Left ventricular papillary muscles were isolated from the sham group and four MI groups, fixated with 2% glutaraldehyde in cacodylate buffer. The left ventricular papillae muscle was separated from the sham operation group and the 4 MI groups and was soaked in lactic acid buffer with 2% glutaraldehyde (mM: 150 Na-cacodylate, 2CaCl2, pH 7.3) for 1 h, then soaked in lactic acid buffer with 1% osmium tetroxide for 30 min, and stained with 1% uranyl acetate solution. After gradient dehydration with ethanol and acetone, the tissues were embedded in Durcupan.

The AC16 cell culture and oxygen-glucose deprivation (OGD) model

AC16 cells (BeNa Culture Collection, Henan, China) were cultured in DMEM (BasaMedia, Shanghai, China) medium containing 10% fetal bovine serum and incubated at 37°C, 5% CO2, and 5% O2 for 24 h.

In an anaerobic chamber gassed with 1% O2, 5% CO2, and 94% N2, AC16 cells were exposed to OGD for 4 h by replacing the complete culture medium to glucose-free culture medium. The successful establishment of OGD model detected by HIF-1α.

Cell transduction

AC16 cells were seeded into each well of a 6-well plate and transduced with empty vector lentivirus and lentivirus with RBM25-GFP respectively (Hanbio, Shanghai, China) in 2 ml low sugar medium containing 7 μg/ml polybrene (MOI:30 Hanbio, Shanghai, China) at 37 °C for 72 h. The cells were then cultured in DMEM containing 10% FBS and 6 μg/ml puromycin for 48 h. The medium changed every 48 h for 2 weeks to obtain RBM25 overexpressing stable transfectant strain (Lent-RBM25 group) and lentiviral empty vector stable transfectant strain (Lent-Ctr group). Stable transfection cell lines with overexpression of RBM25 (Lent-RBM25 group) and lentivirus empty vector (Lent-Ctr group) were obtained by changing the medium every 48 h for 2 weeks. There was no abnormality in the distribution of A/T/G/C content in the sequencing quality assessment in the Lent-RBM25 group and the Lent-Ctr group.

Cell transfection

The small interfering RNA (siRNA) duplexes corresponding to RBM25 siRNA and the negative control siRNA (Control + siRNA) were purchased from Anhui General Biotechnology, Inc. RBM25 siRNA (100 nM) was transfected into AC16 cells using Lipofectamine 6000 transfection reagent (Beyotime, Shang Hai, China) according to the manufacturer's protocol. Briefly, AC16 cells were seeded into a 6-well plate and cultured for 24 h. When the cell density reached 80% confluence, lipofectamine 6000 was added to the serum-free medium and incubated at room temperature for 5 min. The diluted siRNA was mixed with serum-free medium containing lipofectamine 6000, incubated at room temperature for 20 min, and then added to the cell mixture in each well. The transfected cells were incubated at 37 °C in a humidified incubator with 5% CO2 for 72 h before further analysis. Cells transfected with Control + siRNA were used as a negative control. The transfection efficiency of siRNA was measured using Western blot analysis.

Transcriptome sequencing and differential gene expression analysis

Transcriptome sequencing was performed on RBM25 over-expressing stable transfectant strain and lentiviral empty

vector stable transfectant one. Cell suspension was collected when the two cell lines grew to 80–90% fusion and was immediately frozen in liquid nitrogen for about 10s and then stored in dry ice and sent to Shanghai Applied Protein Technology Company (Shanghai, China) for sequencing. The workflow was roughly as follows: Illumina high-throughput sequencing was used to obtain raw sequencing data. Quality assessment was performed by examining the distribution of A/T/G/C content of the raw data, and the HISAT2 software was used at the same time to analyze the alignment with the reference genome. Differential expression analysis of genes was performed using DESeq2, and the difference was considered significant when $P < 0.05$ and |log2foldchange| > 1. Venn diagrams were used to analyze the genes that shared differences in expression fragments per kilobase of exon model per million mapped fragments (FPKM) were used to compare the expression of differential genes in each group.

Enrichment analysis and protein interaction network analysis

Differentially expressed genes (DEGs) and apoptosis-related genes (ARGs) were identified by GO annotation and analyzed by R language package. The STRING database was used to conduct Protein-Protein Interaction (PPI) Networks to find potential interaction relationships between the DEGs. The relationship of target genes was verified using the online database EVEX.

RT-Qpcr

Total RNA was isolated from AC16 cells using Trizol Reagent (Cwbio, Jiangsu, China). The isolated RNA was then reverse transcribed into cDNA. Real-time Qpcr (RT-Qpcr) was performed with the SYBR Green kit (Cwbio, Jiangsu, China) and the CFX96 Real-Time PCR System (BIO-RAD, CA, USA). B-actin was used as an internal control. The mRNA level of each sample was evaluated using the ΔΔCT method. The primer sequences are listed below: RBM25-forward: TGTCTTTTCCACCTCATTTGAATCG, reverse: ATTGGTACAGGAATCATTGGGGT; β-actin -forward: GGATCGGCGGCTCCAT, reverse: CATACTCCTGCT TGCTGATCCA.

Western blotting

Whole-cell lysates were prepared. Total proteins were collected by centrifugation and then quantified by the BCA method (Solarbio, Beijing, China). To run SDS-PAGE, equal amounts of total proteins were loaded onto 10% SDS gels. After electrophoresis, proteins were transferred onto nitrocellulose membranes and blocked in 5% skim milk at 4 °C overnight. The membranes were washed and then incubated at room temperature for 2 h with primary antibodies against RBM25 (1:2500, Abcam, Cambridge, UK), CHOP (1:1000, Abcam, Cambridge, UK), Hif1α (1:1000, Abcam, Cambridge, UK), GAPDH (1:10000, Proteintech, Wuhan, China), BBC3 (1:10000, Proteintech, Wuhan, China), P53 (1:10000, Proteintech, Wuhan, China), and β-tubulin(1:10000, Abmart, Shanghai, China). Subsequently, the membranes were incubated with 4000-fold diluted secondary antibodies (Proteintech, Wuhan, China). Finally, the proteins were detected with an ECL detection kit (NCM Biotech, Suzhou, China) and visualized using the MINICHEML 610, CHAMPGEL6000 (Sage Creation, Beijing, China).

ER localization

ER staining was performed according to the instructions of ER-Tracker Blue kit. After treatment, AC16 were washed twice with PBS and then incubated in pre-warmed ER-tracker dye solution (1 μM) for approximately 15 min at 37 °C. The cells were then observed using a confocal microscopy (Carl Zeiss, Oberkochen, Germany).

Apoptosis analysis

Cells were collected, washed twice with cold PBS buffers, re-suspended with binding buff (BD Biosciences, New Jersey, USA/Muti science, Hangzhou, China), and density adjusted. Cell transfection status was then assessed on flow cytometry (BD Biosciences, NJ, USA) green fluorescent protein (GFP) channels. Cell apoptosis was detected 100 μl cell suspension was mixed with 5 μl AV/APC solution, then again mixed with 5 μl 7-AAD solution, and incubated in the dark for 15 min. Finally, 400 μl binding buff was added and mixed, and the apoptosis rate of the cells was detected by flow cytometry within 1 h.

Statistical analysis

The data were obtained from 5 independent experiments for in vitro studies and six animals in every experimental group for in vivo studies. SPSS 26 software was used for statistical analysis, and Graph prims 8.0 (GraphPad Software, USA) was used for plotting. The data were presented as the mean ± standard deviation (x ± S). All data were compared by Student's *t* test between the two groups. One-way ANOVA was used to compare the differences among three groups. $P < 0.05$ were considered statistically significant.

Results

Myocardial injury in ischemic HF rats

In order to investigate the role of RBM25 in ischemic HF, we induced MI in SD rats. After 2 and 4 weeks of myocardial infarction, the rats in both groups showed significant cardiac dysfunction. We assessed cardiac function by echocardiography (Fig. 1A) and BNP. Echocardiography of rats' hearts demonstrated that LVEDV, LVESV, LVEDD, LVESD (Fig. 1B), and BNP (Fig. 1C) increased in the model group compared with the sham; however, LVEF and FS decreased. Consistent with the cardiac dysfunction, the model group also showed histological damage. H&E staining and Masson's trichrome staining were used to assess myocardial injury**.** In the sham operation group, the myocardial cells were arranged neatly, the nuclei were obvious, and there was no inflammatory cell infiltration. In the ischemic HF group, the myocardial tissue showed extensive myocardial cell necrosis and disordered myocardial fiber arrangement, and a large number of inflammatory cells infiltrated (Fig. 1D). In addition, Masson's trichrome staining results clarified that the sham group was dominated by cardiomyocytes without obvious collagen components; in contrast, myocardial fibrosis was evident in the ischemic HF group, with only a few remaining cardiomyocytes (Fig. 1E and F). Furthermore, transmission electron microscopy examination revealed an expanded ER lumen in the myocardium of ischemic HF rats (Fig. 1G). These results indicate that cardiac function and myocardial cells are significantly impaired in ischemic HF rats.

RBM25 is elevated in hypoxic-injured cardiomyocytes

As the duration of HF prolonged, the expression of RBM25 significantly increased in the ischemic HF group. RBM25 was quantified and localized through Western blot and immunofluorescence. Western blot results showed that RBM25 protein levels in the ischemic HF group were significantly higher than those in the sham control group both in vivo (Fig. 2A and B) and in vitro (Fig. 2D and E). The elevated RBM25 was mainly localized in the nucleus of cardiomyocytes by co-localization with cardiac troponin T (Fig. 2C and F). Thus, when ischemic HF occurs, RBM25 expression levels located in the myocardial nucleus are significantly elevated.

Overexpression of RBM25 in AC16 promotes apoptosis

To explore the role of RBM25 in the progression of HF, we first overexpressed RBM25 in cardiomyocytes using lentiviral transfection and validated it by flow cytometry and RT-PCR. Flow cytometry showed that 90% of the cells carried GFP (Fig. 3A). The expression of RBM25 was significantly elevated in Lent-RBM25 group (Fig. 3B). We then used flow cytometry to detect cell apoptosis. Apoptosis of Lent-RBM25 group increased significantly (apoptosis rate was 28.49%) compared with Lent-Ctr group (Fig. 3C and D). Therefore, overexpression of RBM25 could induce cell apoptosis.

Transcriptome sequencing and differential gene screening

The number of sequencing sequences that could be mapped to the reference genome exceeded 90%. By comparing the sequencing results of Lent-RBM25 group and Lent group, the differential genes were obtained (Fig. 4A). The possible downstream pathways of RBM25 were then identified by GO enrichment analysis and protein interaction analysis. GO enrichment analysis showed that the most prominent biological processes, molecular functions, and cell compositions involved in these differenced genes were response to unfolded proteins, misfolded proline binding, and CHOP, respectively (Fig. 4B). Analysis of the function and expression of the corresponding genes interacting with CHOP showed that the pro-apoptotic genes PPP1R15A and BBC3 were increased (Fig. 4C). The EVEX online database found that BBC3 was regulated by CHOP. These results suggest that RBM25 may play a role through the ER stress related pathway CHOP/BBC3, thereby mediating apoptosis.

RBM25 enhances ER stress response through CHOP-associated ER stress pathway signaling

We validated the CHOP/BBC3 pathway predicted by bioinformatics analysis in RBM25 overexpressed cells and OGD model, respectively. Considering the close connection between ER stress and cell apoptosis, we further evaluated the effects of RBM25 on key molecules involved in the unfolded protein response, CHOP, and BBC3. CHOP and BBC3 were significantly increased in RBM25 overexpressed cells, while P53 was decreased in these cells (Fig. 5A and B). Interestingly, the ER shrinked when RBM25 was overexpressed (Fig. 5C). These results suggest that overexpression of RBM25 may significantly promote myocardial cell apoptosis through CHOP/P53/BBC3/ER stress-related pathways The same phenomenon was observed in the OGD model (Fig. 6A and B), and even the contraction of the ER was more pronounced (Fig. 6C). Hence, RBM25 may mediate apoptosis through CHOP-associated pathways when cardiomyocytes are injured by hypoxia.

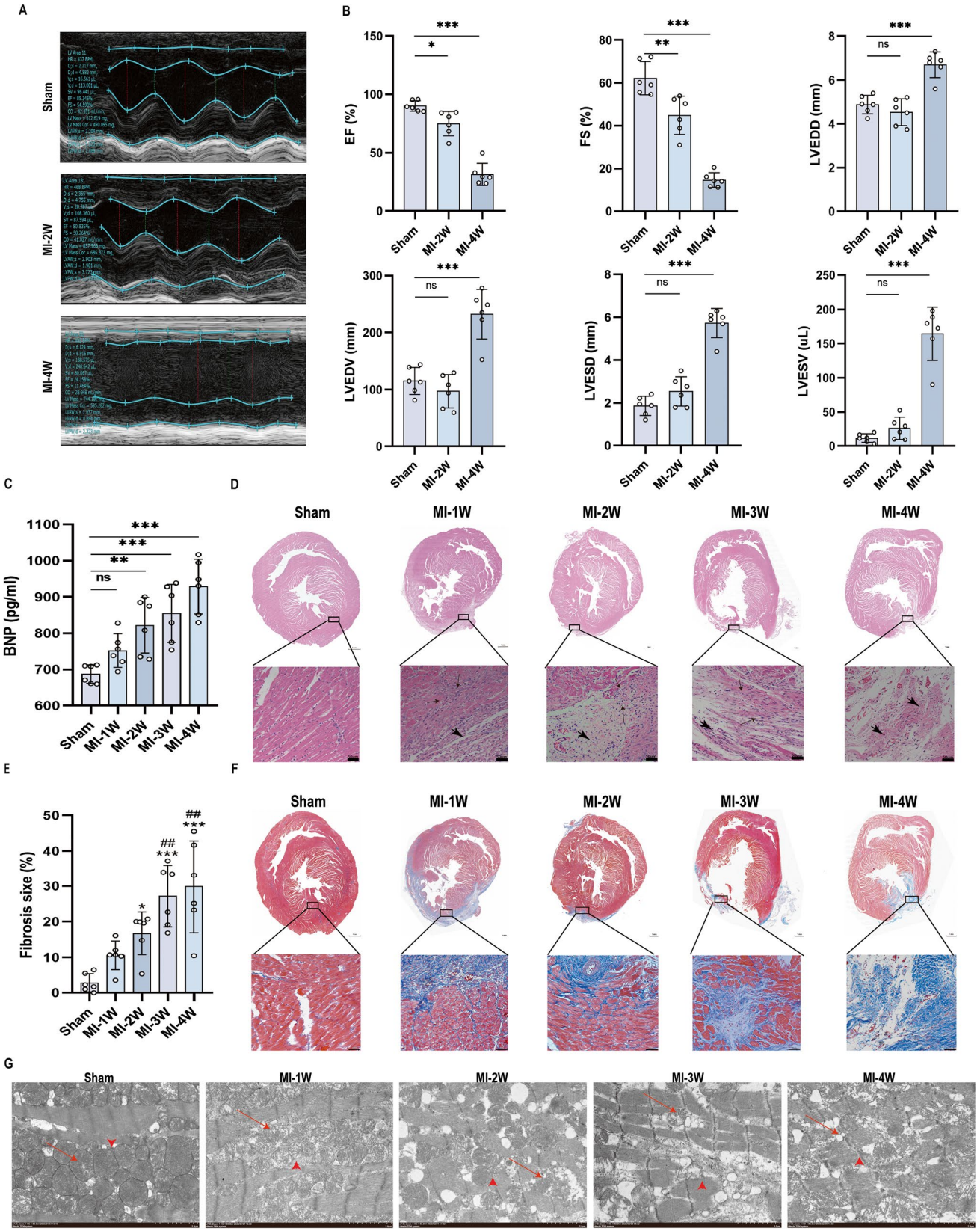
A
Sham
MI-2W
MI-4W
B
EF (%)
FS (%)
LVEDD (mm)
LVEDV (mm)
LVESD (mm)
LVESV (uL)
Sham
MI-2W
MI-4W
ns
C
BNP (pg/ml)
Sham
MI-1W
MI-2W
MI-3W
MI-4W
D
Sham
MI-1W
MI-2W
MI-3W
MI-4W
E
Fibrosis sixe (%)
F
G

◂**Fig. 1** Myocardial infarction induces heart failure in rats. **A**, **B** Echocardiography and quantized histogram of ejection fraction (EF), left ventricular fractional shortening (FS), the left ventricular end-diastolic inner diameter (LVEDD), left ventricular end-diastolic volume (LVEDV), left ventricular end-systolic inner diameter (LVESD), and left ventricular end-systolic volume (LVESV). $n = 6$ rats. **C** Differences in the expression levels of BNP among all groups. **D** Representative images of H&E staining in each group. Arrows indicate different levels of inflammatory cell infiltration. Arrows heads indicate different levels of fibrocyte infiltration in the ischemic area (scale bar: 50 μm). **E**, **F** Representative Masson staining images and quantitative data in each group: red section, myocardium; blue section, scarred fibrosis (scale bar: 50 μm). **G** The endoplasmic reticulum ultrastructure of left ventricular papillary muscle cells observed by transmission electron microscopy. Images (scale bar: 2 μm) highlighted the ER structure pointed by arrows heads and mitochondrial autophagy by arrows. Data are expressed as mean ± SD. $^{*}P < 0.05$, $^{**}P < 0.01$, $^{***}P < 0.001$ vs. the Sham group. $^{\#\#}P < 0.01$ vs. the MI-1 W group

ER stress can activate expression of RBM25

We further explored how exactly does RBM25 mediate cardiomyocyte apoptosis. After interfering RBM25 expression, CHOP, P53, BBC3, and caspase3 protein expression decreased (Fig. 7A and B). When cardiomyocytes were stimulated by ER stress inducer, tunicamycin (Tu), the expressions of RBM25, CHOP, and BBC3 increased, then interfered with the expressions of RBM25, and the expressions of CHOP and BBC3 decreased (Fig. 7C and D). In addition, inhibition of RBM25 reduced CHOP-related signaling pathways. The above results indicate that ER stress could activate RBM25/CHOP/BBC3 pathway to mediate cardiomyocyte apoptosis.

Inhibiting the expression of RBM25 has a protective effect on the myocardium

Finally, the protective effect of knockdown of RBM25 gene in OGD model was evaluated. As expected, we found that expression of CHOP, P53, BBC3, and Caspase3 decreased in RBM25 siRNA group of OGD model (Fig. 8A and B). Myocardium cell apoptosis of RBM25 siRNA group decreased significantly compared with the control siRNA and control group (Fig. 8C and D). Therefore, inhibiting the expression of RBM25 may effectively inhibit myocardial cell apoptosis. Considering that RBM25 deficiency can inhibit apoptosis, we hypothesized that reducing RBM25 levels may improve cardiac function in ischemic HF model. To test this idea, we evaluated cardiac function in ischemic HF model after RBM25 gene knockdown by echocardiography (Fig. 9A). The results showed that LVESV and LVESD were decreased and LVEF and FS were significantly increased in the MI + shRBM25 group compared with the other two groups (Fig. 9B). Foreseeable, RBM25 may become a new therapeutic target for ischemic HF.

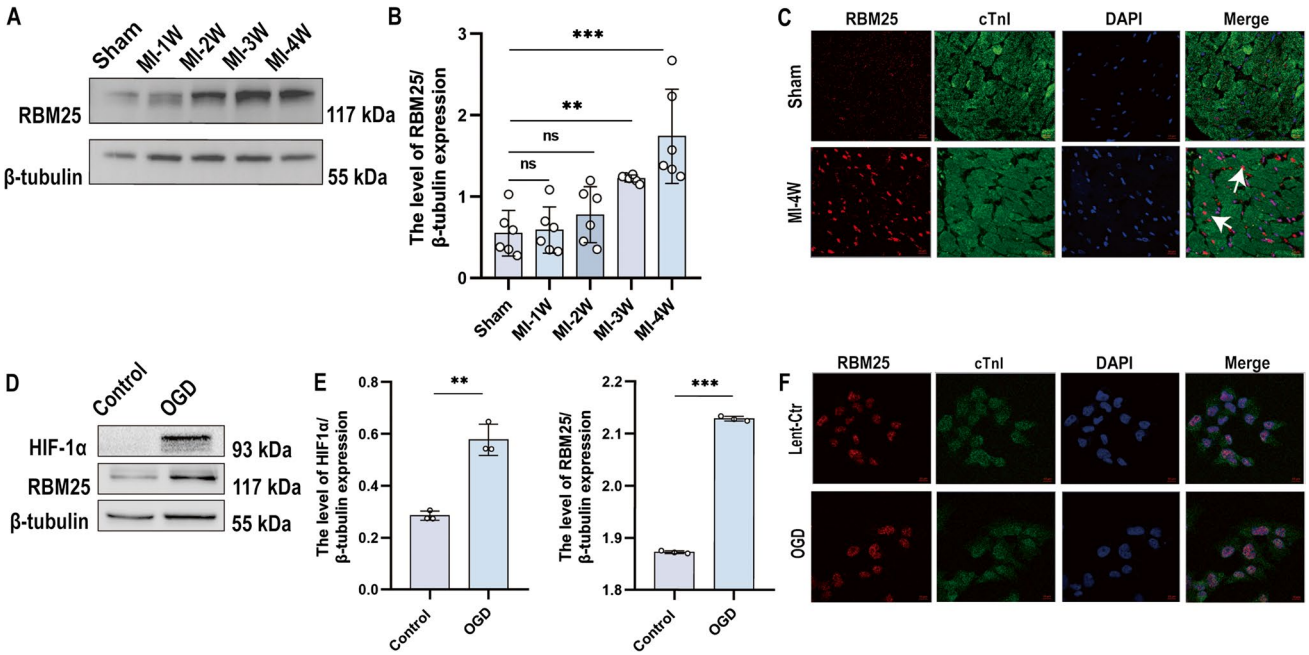

Fig. 2 RBM25 is elevated and localized in nucleus. **A**, **B** Western Blot results and quantization histograms of RBM25 expression in rats of each group. **C** Immunofluorescence images of myocardial tissue of rats in Sham group and MI-4 W group. The red fluorescence represents RBM25, the green fluorescence represents cardiac troponin I (cTnI), and the blue fluorescence represents the nucleus stained by DAPI (scale bar: 10 μm). **D**, **E** Western Blot results and quantization histograms of RBM25 and HIF1-α expression in each group of AC16. **F** Immunofluorescence images of AC16 in Lent-Ctr group and OGD group. The red fluorescence represents RBM25, the green fluorescence represents cardiac troponin I (cTnI), and the blue fluorescence represents the nucleus stained by DAPI (scale bar: 10 μm). Data are expressed as mean ± SD. $^{**}P < 0.01$, $^{***}P < 0.001$ vs. the sham group/control group. OGD, oxygen-glucose deprivation

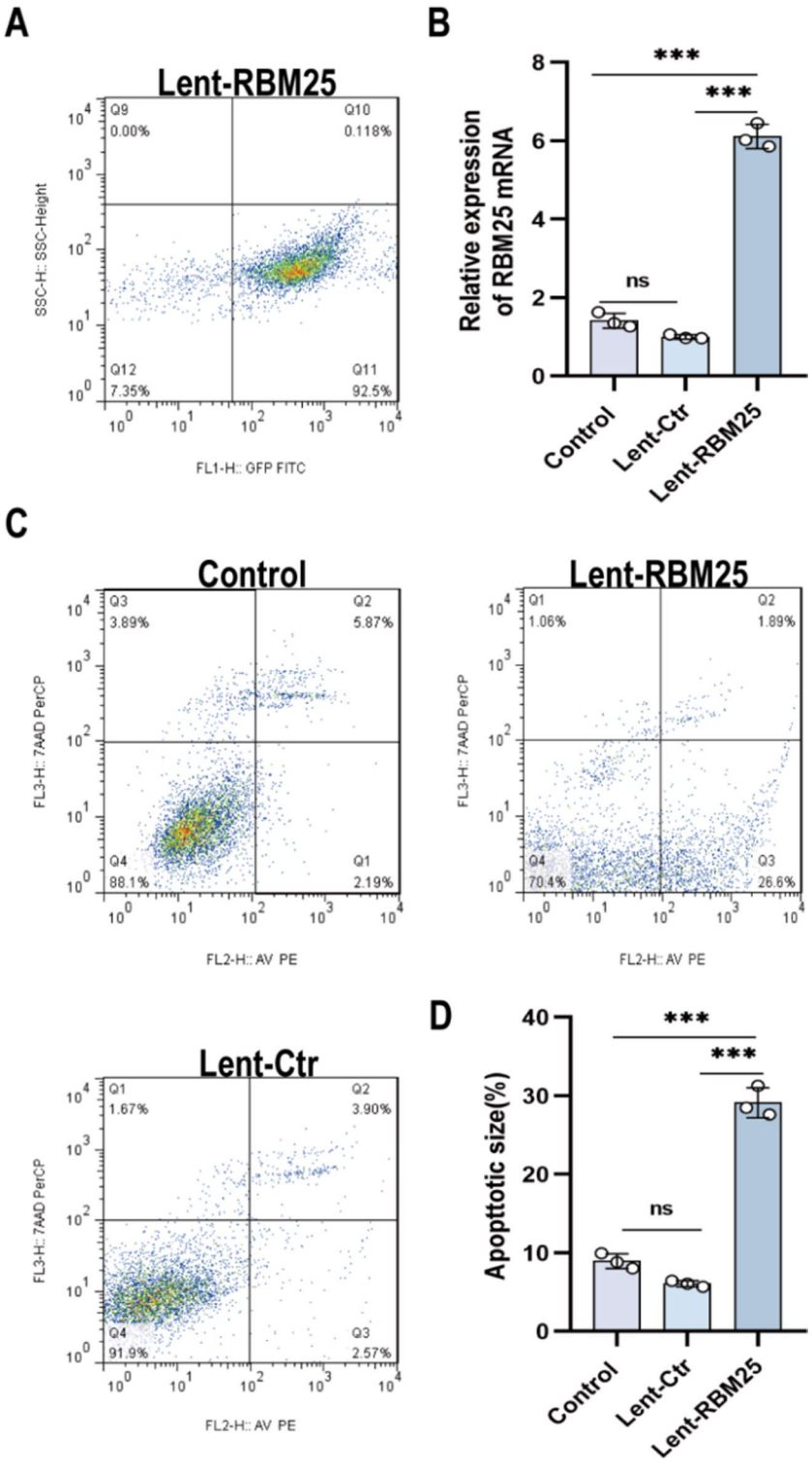

Fig. 3 Overexpression of RBM25 could induce cell apoptosis. **A** Flow cytometry was used to determine the transfection efficiency of GFP fluorescent label in RBM25-overexpression group. **B** PCR results of RBM25 mRNA in each group. **C**, **D** Flow cytometry of apoptosis in each group. ***$P < 0.001$ vs. the control/Lent-Ctr group

Discussion

Apoptosis is an important mechanistic process in the pathological damage of HF [14; 15; 16]. In Olivetti et al.'s study, 39 HF heart samples showed a 232-fold increase in apoptotic cardiomyocytes with morphological changes compared to 11 normal heart tissues (Olivetti et al. 1997). Apoptosis can occur during myocardial cell injury (Shi et al. 2021). The pathological process of myocardial apoptosis in patients with HF is closely related to MI and hypoxia injury[19; 20; 21]. Although ER stress has been proven to be an important mechanism of HF pathology, the

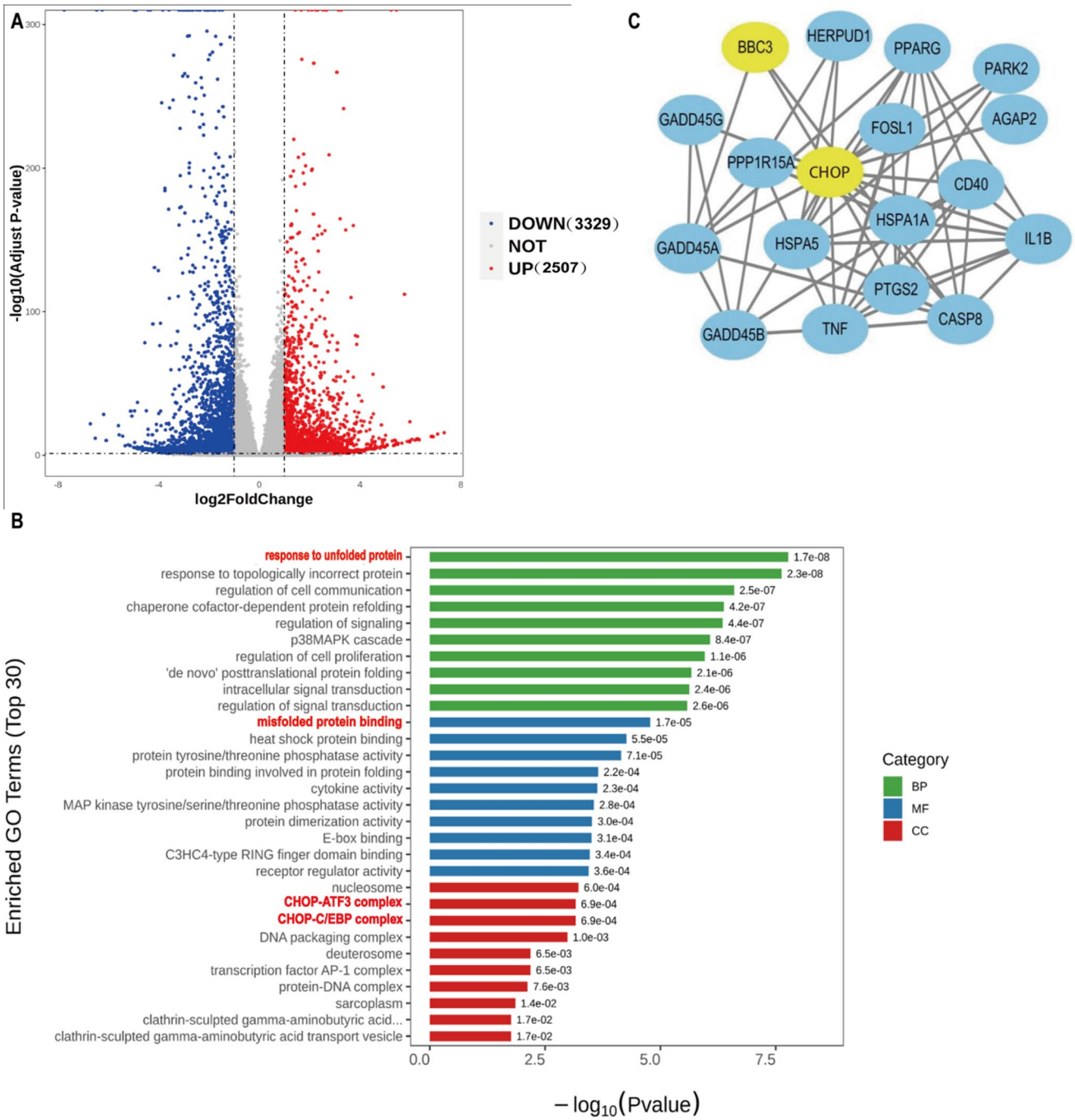

Fig. 4 Sequencing analysis of RBM25 related genes. **A** Volcanic plot of differential genes between Lent-Ctr group and Lent-RBM25 group. Genes with logFC > 1 are considered to have significant differences, and *P* values < 0.05 are considered to have statistically significant differences. **B** The top 30 terms of GO enrichment analysis of selected differential genes. **C** PPI analysis of CHOP protein. GO, Gene Ontology; PPI, protein-protein interaction

relationship between ER stress and cardiomyocyte apoptosis remains unclear. Compelling evidence reports that ER stress can mediate increased apoptosis of cardiomyocytes (Yuan et al. 2020). Some studies indicate that ER stress trigger apoptosis to clear misfolded proteins and even impaired organelles attenuating damage and promoted homeostasis in cells (Garufi et al. 2020). However, other studies show that ER stress trigger apoptosis in HF.

RBM25 is an RNA-binding protein (Xiao et al. 2019). Studies have shown that RBM25 can be involved in the regulation of tumor cell apoptosis [28; 29], and RBM25 is increased in human HF heart (Gao et al. 2011), but the

specific mechanism of RBM25 regulation of HF cell apoptosis has not been reported so far. In this study, we found that RBM25 aggravated the pathological process of HF by regulating ER stress-mediated apoptosis, and downregulating RBM25 reversed apoptosis-mediated cardiac dysfunction. RBM25 levels were significantly increased in OGD models of AC16 cells and in myocardium of HF rats. Based on transcriptome sequencing data, we hypothesized that RBM25 was involved in apoptosis through the CHOP/BBC3 branch of the ER stress response. To verify this prediction, RBM25 was overexpressed or knocked down in AC16 cells, and the expression of key molecules in CHOP-associated pathways was found to be altered. In addition, downregulation of RBM25 alleviates ER dysfunction and apoptosis in the OGD model and improves cardiac function in the ischemic HF model, providing evidence that RBM25 may regulate apoptosis through CHOP-related pathways. YY1, a known RNA-dependent transcription factor, has been found to be a structural regulator of enhancer-promoter loops (Weintraub et al. 2017) and to specifically enhance the transcriptional activation of the GRP78 promoter under various of ER stress conditions (Outinen et al. 1999). In view of the extensive co-binding of YY1 and RBM25, the two proteins regulate a large number of common genes at the transcriptional level, and RBM25 first acts on the targeted promoter of YY1, providing necessary conditions for the subsequent binding of YY1 (Xiao et al. 2019). Therefore, RBM25 may regulate the expression of CHOP through YY1 and promote apoptosis. When ischemic or dilated cardiomyopathy occurs, an increase in RBM25 is thought to be caused by excess angiotensin II or hypoxia. This is consistent with our findings. Furthermore, knockdown RBM25 can inhibit cardiomyocyte apoptosis and improve cardiac function. Thus, intervention of the above processes may prevent adverse cardiac progression and myocardial cell damage in ischemic HF, and the specific mechanisms involved need to be further studied.

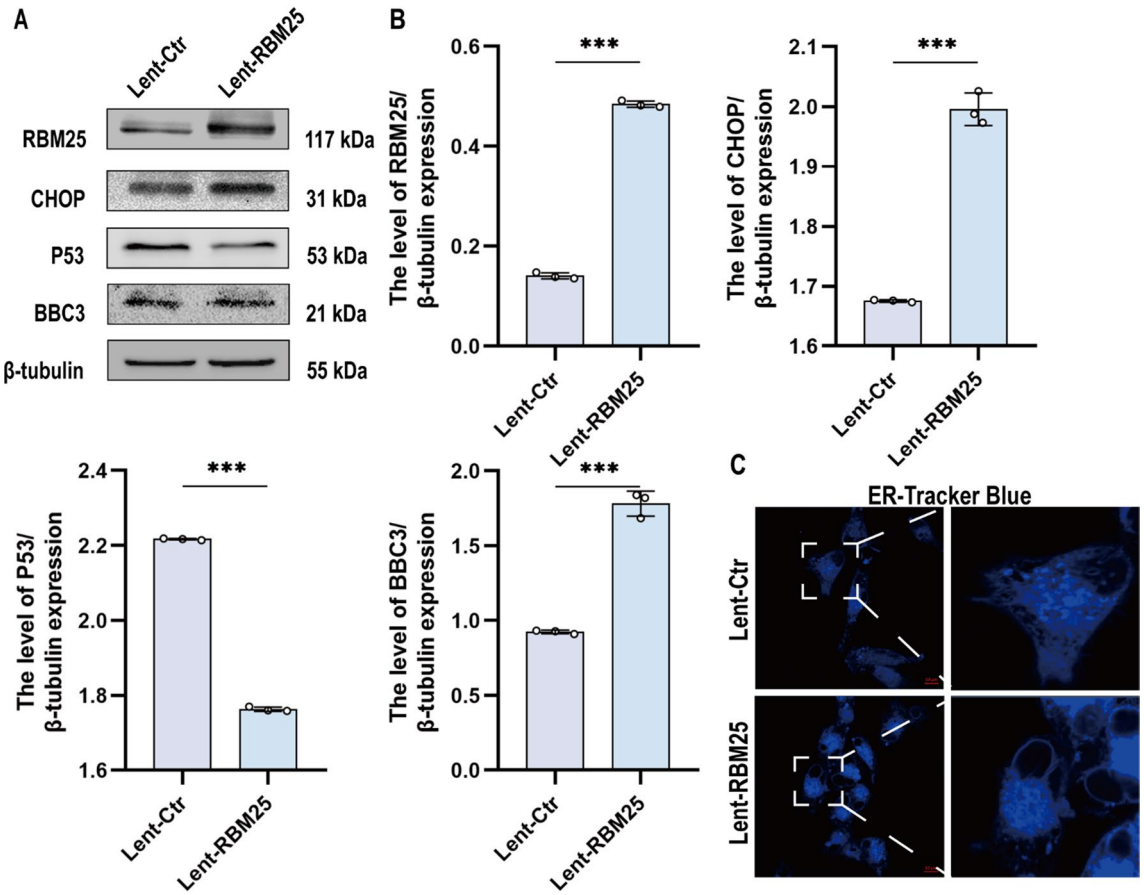

Fig. 5 Overexpression of RBM25 significantly promotes the CHOP/P53/BBC3 pathway associated with ER stress. **A**, **B** Western Blot results and quantization histograms of RBM25, CHOP, P53, and BBC3 expression in each group of AC16. **C** Lent-Ctr group and Lent-RBM25 group were stained with ER-Tracker Blue (1 uM, 15 min) at 37 °C. The cells were then washed with PBS and visualized by confocal microscopy (scale bar: 10 μm). Data are expressed as mean ± SD. ***$P < 0.001$ vs. the Lent-Ctr group

BBC3 as a downstream target gene of CHOP plays an important role in ER stress-induced apoptosis [34; 35; 36]. BBC3 encodes a BH3-only protein, a pro-apoptotic member of the Bcl-2 family required to initiate apoptosis and is a key mediator of the P53-induced apoptotic response (Villunger et al. 2003). DNA damage stimuli trigger P53 transcriptional responses, resulting in the upregulation of target gene BBC3. $BBC3^{BH3}$ binds to Bcl-Xl at the canonical binding site, promotes the release of P53 upon dissociation, and activates pro-apoptotic Caspase 3 to promote P53-dependent apoptosis (Xing et al. 2016). Therefore, we are interested in whether CHOP regulates BBC3 through P53.

Our studies demonstrate that BBC3 expression may be important for the cardiomyocyte apoptotic process and can be transcriptionally induced by ER stress. Compared with normal cardiomyocytes, the expressions of CHOP, BBC3, and P53 were significantly upregulated after RBM25 overexpression, and all were downregulated after RBM25 knockdown. Interestingly, in OGD model, the elevated RBM25 was accompanied by the upregulation of CHOP, BBC3, and HIF1α, but the expression of P53 was significantly downregulated. P53 accumulation has been shown to interfere with hypoxia-sensing systems and promote proteasomal degradation of HIF1α, resulting in impaired cardiac angiogenesis and left ventricular dysfunction (Gogiraju et al. 2015). This is consistent with our study, in which we found that when HIF1αis upregulated, it can interfere with P53 expression. The hypoxia of AC16 cardiomyocytes led to the increase of RBM25, while the downregulation of P53 was associated with the increase of HIF1α level induced by hypoxia. This implies that the interaction between HIF1αand P53 may have important implications for the stability of the cardiovascular system. Therefore, we suggest that RBM25 regulates CHOP/BBC3 ER stress response-mediated apoptosis independent of p53.

We established the OGD model of AC16 cardiomyocytes, which was mainly used to simulate the important pathological mechanism of ischemia and hypoxia in HF. The expression of RBM25 was significantly upregulated, and apoptosis was significantly increased after oxygen glucose deprivation.

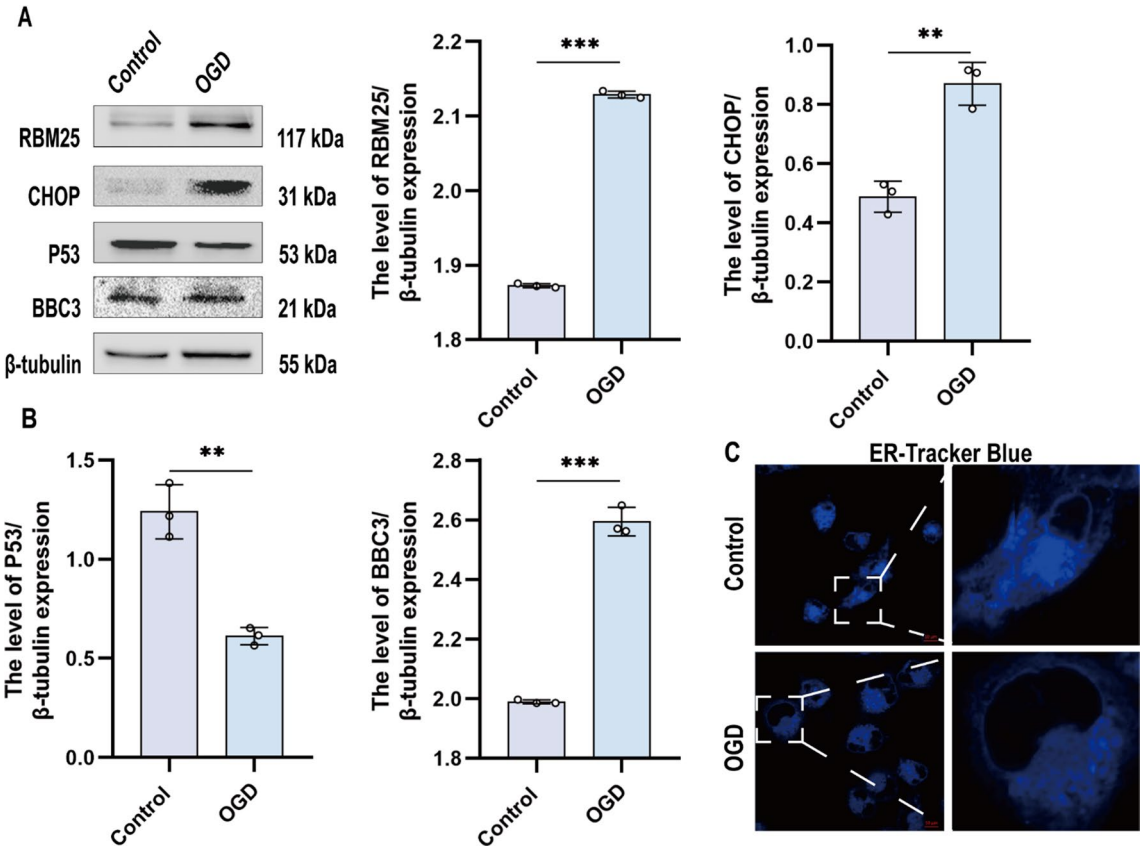

Fig. 6 RBM25 could mediate ER stress in OGD models through CHOP/P53/BBC3 in pathway. **A**, **B** Western Blot results and quantization histograms of RBM25, CHOP, P53, and BBC3 expression in each group of AC16. C The control and OGD groups were stained with ER-Tracker Blue (1 uM, 15 min) at 37 °C. The cells were then washed with PBS and visualized by confocal microscopy (scale bar: 10 μm). Data are expressed as mean ± SD. $^{**}P < 0.01$, $^{***}P < 0.001$ vs. the control group. OGD, oxygen-glucose deprivation

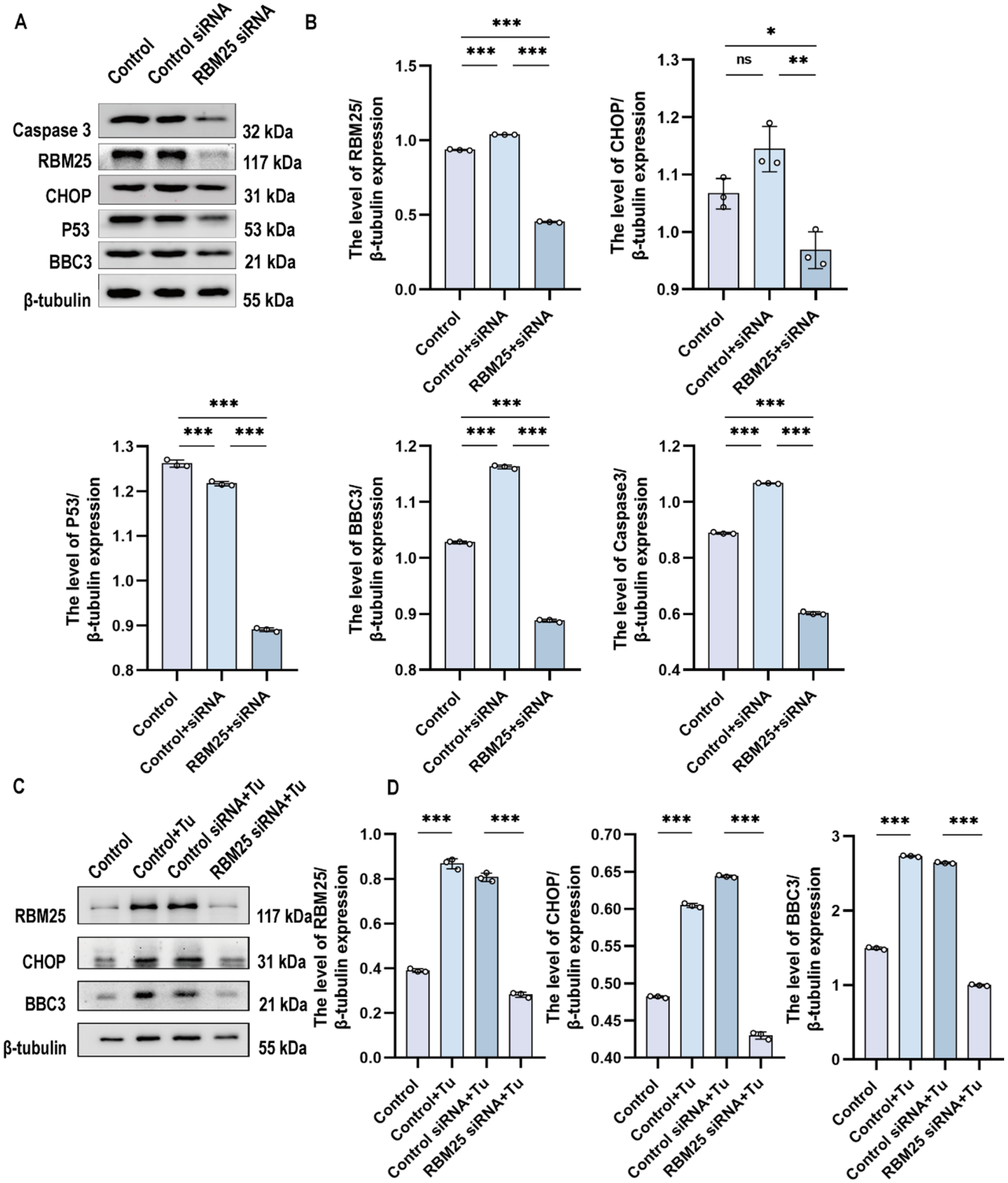

Fig. 7 ER stress could activate RBM25 to mediate cardiomyocyte apoptosis. **A**, **B** Western blot results and quantization histograms of RBM25, CHOP, P53, BBC3, and Caspase3 expression in each group. **C**, **D** Western blot results and quantization histograms of RBM25, CHOP, and BBC3 expression in each group of AC16. Data are expressed as mean ± SD. $^{*}P < 0.05$, $^{**}P < 0.01$, $^{***}P < 0.001$ vs. the control/control+siRNA/control siRNA+Tu group. Tu, tunicamycin

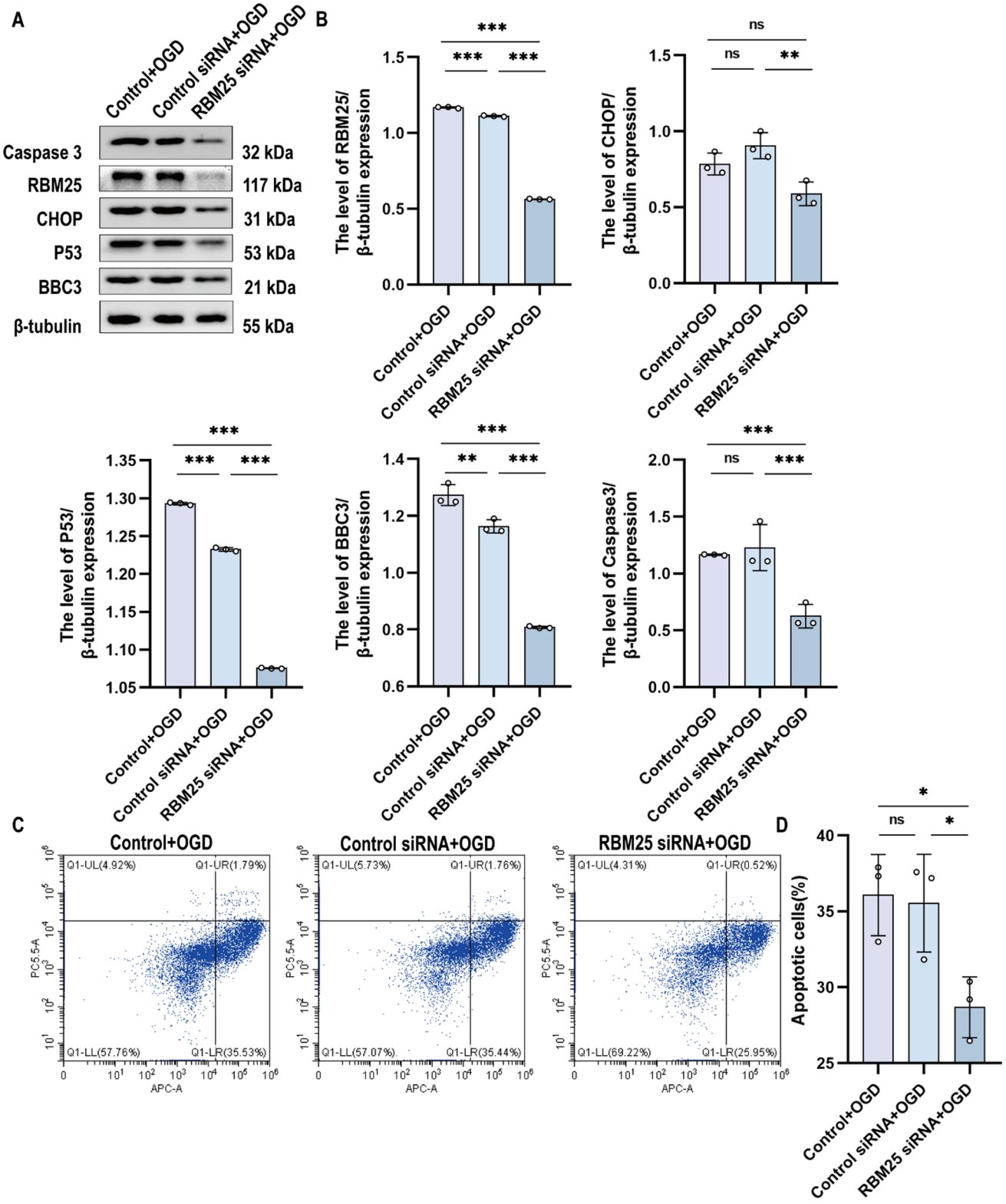

Fig. 8 Inhibiting the expression of RBM25 has a protective effect in vitro. **A**, **B** Western blot results and quantization histograms of RBM25, CHOP, P53, BBC3, and Caspase3 expression in each group. **C**, **D** Flow cytometry of apoptosis in each group. Data are expressed as mean ± SD. $^{*}P < 0.05$, $^{**}P < 0.01$, $^{***}P < 0.001$ vs. the control+OGD/control siRNA25 + OGD group. OGD: oxygen-glucose deprivation

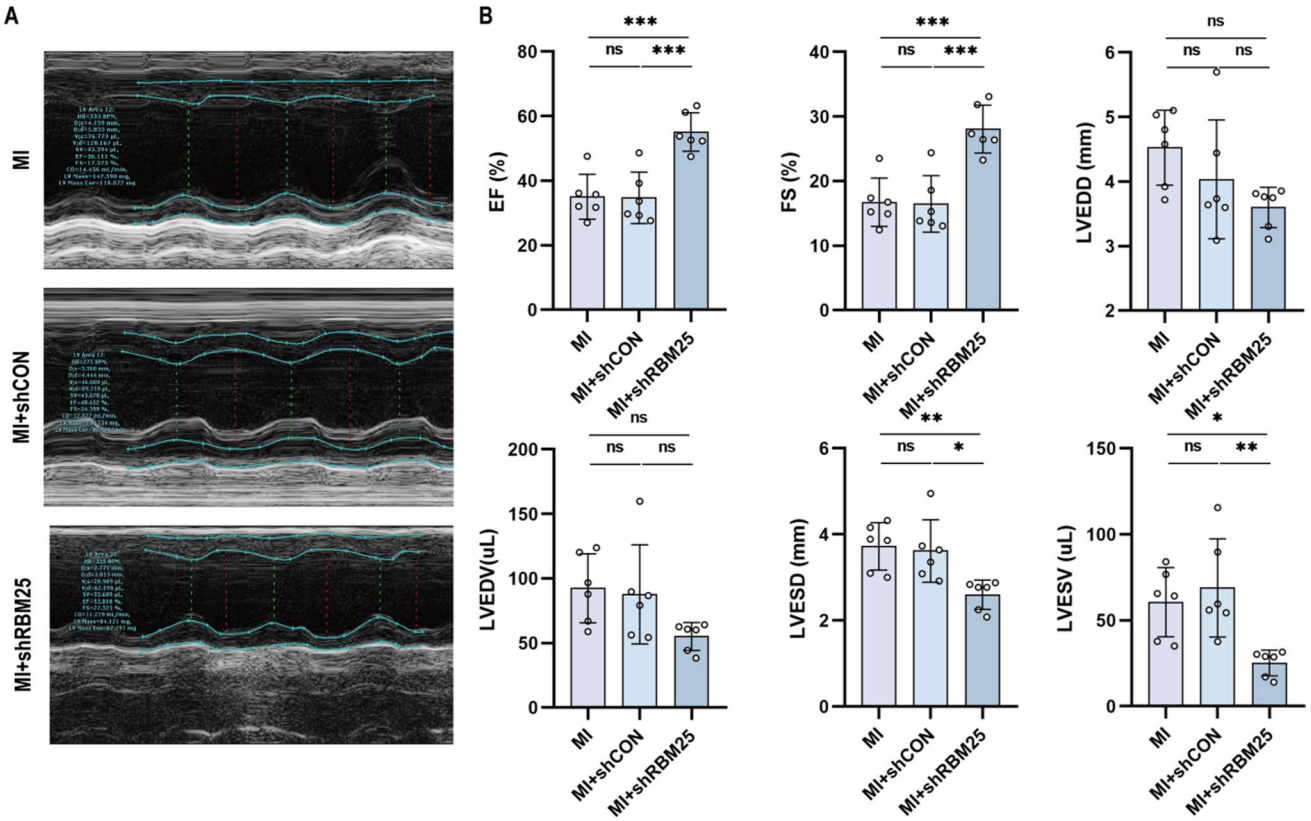

Fig. 9 Inhibiting the expression of RBM25 has a protective effect in vivo. **A**, **B** Echocardiography and quantized histogram of ejection fraction (EF), left ventricular fractional shortening (FS), left ventricular end-diastolic inner diameter (LVEDD), left ventricular end-diastolic volume (LVEDV), left ventricular end-systolic inner diameter (LVESD), and left ventricular end-systolic volume (LVESV). $n = 6$ mice

Interestingly, CHOP-associated pathways were expressed in the same direction. When RBM25 was knocked down, the expression of CHOP pathway–related proteins was reduced, and cell apoptosis and cardiac function injury were significantly improved.

This study has some limitations. Although BBC3 is a pro-apoptotic member of the Bcl-2 family required to initiate apoptosis, further exploration of its relationship with Bax and Bcl-2 is needed. In addition, the specific mechanism of ER stress leading to the rise of RBM25 remains unclear. In the future, we will study the crosstalk between RBM25 and ER stress.

In conclusion, RBM25 is significantly upregulated in the OGD model and HF rat heart and leads to apoptosis by regulating CHOP-related pathways of ER stress response. Knockdown of RBM25 was able to reverse the adverse outcomes of ER stress. Therefore, targeting RBM25 may be an effective strategy to alleviate the adverse consequences of ER stress in HF, thus providing a new theoretical basis and new ideas for the treatment of HF.

Acknowledgements We thank the National Natural Science Foundation of China for funding this work.

Funding This work was supported by the National Natural Science Foundation of China (grant numbers NSFC,82060080), Gansu science and Technology Department Project (20YF3WA016), Gansu Provincial Department of education project (2020B-024), Project of Lanzhou science and Technology Bureau (2019-RC36), and the Cuiying Scientific and Technological Innovation Program of Lanzhou University Second Hospital (CY2022-MS-A06). This study was also supported by Gansu heart rehabilitation engineering research center (CRQI-C00535).

Data availability The data that support the findings of this study are available on request from the corresponding author. The data are not publicly available due to privacy restrictions.

Declarations

Conflict of interest The authors declare no competing interests.

References

Akazawa Y, Cazanave S, Mott JL, Elmi N, Bronk SF, Kohno S, Charlton MR, Gores GJ (2010) Palmitoleate attenuates palmitate induced Bim and PUMA up-regulation and hepatocyte lipoapoptosis. J. Hepatol 52:586–593

Baer A, Lundberg L, Swales D, Waybright N, Pinkham C, Dinman JD, Jacobs JL, Kehn-Hall K (2016) Venezuelan equine encephalitis virus induces apoptosis through the unfolded protein response activation of EGR1. Virol. J 90:3558–3572

Bagheri-Yarmand R, Dadu R, Ye L, Shiny Jebaraj Y, Martinez JA, Ma J, Tarapore RS, Allen JE, Sherman SI, Williams MD, Gagel RF (2021) ONC201 shows potent anticancer activity against medullary thyroid cancer via transcriptional inhibition of RET VEGFR2 and IGFBP2. Mol. Cancer Ther 20:665–675

Baumeister P, Luo S, Skarnes WC, Sui G, Seto E, Shi Y, Lee AS (2005) Endoplasmic reticulum stress induction of the Grp78 BiP promoter activating mechanisms mediated by YY1 and its interactive chromatin modifiers. Mol. Cell. Biol 25:4529–4540

Cao JW, Tang ZB, Zhao JW, Zhao JK, Yao JL, Sheng XM, Zhao MQ, Duan Q, Han BC, Duan SR (2022) LncRNA nuclear enriched abundant transcript 1 aggravates cerebral ischemia reperfusion injury through activating early growth response 1 RNA binding motif protein 25 axis. J. Neurochem 163:500–516

Carlson SM, Soulette CM, Yang Z, Elias JE, Brooks AN, Gozani O (2017) RBM25 is a global splicing factor promoting inclusion of alternatively spliced exons and is itself regulated by lysine mono methylation. J Biol Chem 292:13381–13390

Castiglione V, Aimo A, Vergaro G, Saccaro L, Passino C, Emdin M (2022) Biomarkers for the diagnosis and management of heart failure. Heart Fail. Rev 27:625–643

Feng H, Mou SQ, Li WJ, Zhang N, Zhou ZY, Ding W, Bian ZY, Liao HH (2020) Resveratrol inhibits ischemia induced myocardial senescence signals and NLRP3 inflammasome activation. Oxid. Med. Cell. Longev. OXID MED CELL LONGEV 2020:2647807

Feuerstein G, Yue TL, Ma X, Ruffolo RR (1998) Novel mechanisms in the treatment of heart failure inhibition of oxygen radicals and apoptosis by carvedilol. Prog Cardiovasc Dis 41:17–24

Gao G, Xie A, Huang SC, Zhou A, Zhang J, Herman AM, Ghassemzadeh S, Jeong EM, Kasturirangan S, Raicu M, Sobieski MA 2nd, Bhat G, Tatooles A, Benz EJ Jr, Kamp TJ, Dudley SC Jr (2011) Role of RBM25 LUC7L3 in abnormal cardiac sodium channel splicing regulation in human heart failure. Circulation 124:1124–1131

Gao G, Chen W, Yan M, Liu J, Luo H, Wang C, Yang P (2020) Rapamycin regulates the balance between cardiomyocyte apoptosis and autophagy in chronic heart failure by inhibiting mTOR signaling. Int J Mol Med 45:195–209

Garufi A, Federici G, Gilardini Montani MS, Crispini A, Cirone M, D'Orazi G (2020) Interplay between endoplasmic reticulum ER stress and autophagy induces mutant p53H273 degradation. Biomolecules 10

Ge Y, Schuster MB, Pundhir S, Rapin N, Bagger FO, Sidiropoulos N, Hashem N, Porse BT (2019) The splicing factor RBM25 controls MYC activity in acute myeloid leukemia. Nature communications 10:172

Gogiraju R, Xu X, Bochenek ML, Steinbrecher JH, Lehnart SE, Wenzel P, Kessel M, Zeisberg EM, Dobbelstein M, Schäfer K (2015) Endothelial p53 deletion improves angiogenesis and prevents cardiac fibrosis and heart failure induced by pressure overload in mice. J Am Heart Assoc 4

Gordon S, Akopyan G, Garban H, Bonavida B (2006) Transcription factor YY1 structure function and therapeutic implications in cancer biology. Oncogene 25:1125–1142

Gustafsson AB, Gottlieb RA (2003) Mechanisms of apoptosis in the heart. J. Clin. Immunol 23:447–459

Heidenreich PA, Bozkurt B, Aguilar D, Allen LA, Byun JJ, Colvin MM, Deswal A, Drazner MH, Dunlay SM, Evers LR, Fang JC, Fedson SE, Fonarow GC, Hayek SS, Hernandez AF, Khazanie P, Kittleson MM, Lee CS, Link MS et al (2022) AHA ACC HFSA Guideline for the Management of Heart Failure: a report of the American College of Cardiology American Heart Association Joint Committee on Clinical Practice Guidelines. Circulation 145(2022):e895–e1032

Hu H, Tian M, Ding C, Yu S (2018) The C EBP homologous protein CHOP transcription factor functions in endoplasmic reticulum stress induced apoptosis and microbial infection. Front. immunol 9:3083

Li M, Feng J, Cheng Y, Dong N, Tian X, Liu P, Zhao Y, Qiu Y, Tian F, Lyu Y, Zhao Q, Wei C, Wang M, Yuan J, Ying X, Ren X, Yan X (2022) Arsenic fluoride co-exposure induced endoplasmic reticulum stress resulting in apoptosis in rat heart and H9c2 cells. Chemosphere 288:132518

Matsumura T, Nakamura-Ishizu A, Muddineni S, Tan DQ, Wang CQ, Tokunaga K, Tirado-Magallanes R, Sian S, Benoukraf T, Okuda T, Asou N, Matsuoka M, Osato M, Suda T (2020) Hematopoietic stem cells acquire survival advantage by loss of RUNX1 methylation identified in familial leukemia. Blood 136:1919–1932

Noyes AM, Zhou A, Gao G, Gu L, Day S, Andrew Wasserstrom J, Dudley SC (2017) Abnormal sodium channel mRNA splicing in hypertrophic cardiomyopathy. Int. J. Cardiol 249:282–286

Olivetti G, Abbi R, Quaini F, Kajstura J, Cheng W, Nitahara JA, Quaini E, Di Loreto C, Beltrami CA, Krajewski S, Reed JC, Anversa P (1997) Apoptosis in the failing human heart. NEJM 336:1131–1141

Omidkhoda N, Wallace Hayes A, Reiter RJ, Karimi G (2019) The role of MicroRNAs on endoplasmic reticulum stress in myocardial ischemia and cardiac hypertrophy. Pharmacol. Res 150:104516

Outinen PA, Sood SK, Pfeifer SI, Pamidi S, Podor TJ, Li J, Weitz JI, Austin RC (1999) Homocysteine-induced endoplasmic reticulum stress and growth arrest leads to specific changes in gene expression in human vascular endothelial cells. Blood 94:959–967

Ren J, Bi Y, Sowers JR, Hetz C, Zhang Y (2021) Endoplasmic reticulum stress and unfolded protein response in cardiovascular diseases. Nat Rev Cardiol 18:499–521

Shan J, Dudenhausen E, Kilberg MS (2019) Induction of early growth response gene 1 EGR1 by endoplasmic reticulum stress is mediated by the extracellular regulated kinase ERK arm of the MAPK pathways. Biochim:371–381

Shi Y, Zhang Z, Yin Q, Fu C, Barszczyk A, Zhang X, Wang J, Yang D (2021) Cardiac specific overexpression of miR 122 induces mitochondria-dependent cardiomyocyte apoptosis and promotes heart failure by inhibiting Hand2. J Cell Mol Med 25:5326–5334

Su Y, Tian H, Wei L, Fu G, Sun T (2018) Integrin β3 inhibits hypoxia-induced apoptosis in cardiomyocytes. Acta biochimica et biophysica Sinica 50:658–665

Takemura G, Kanamori H, Okada H, Miyazaki N, Watanabe T, Tsujimoto A, Goto K, Maruyama R, Fujiwara T, Fujiwara H (2018) Anti apoptosis in nonmyocytes and pro autophagy in cardiomyocytes two strategies against postinfarction heart failure through regulation of cell death degeneration. Heart Fail. Rev 23:759–772

Villunger A, Michalak EM, Coultas L, Müllauer F, Böck G, Ausserlechner MJ, Adams JM, A. (2003) Strasser, p53- and drug-induced apoptotic responses mediated by BH3-only proteins puma and noxa. Science, vol 302, (New York, N.Y.), pp 1036–1038

Wang S, Binder P, Fang Q, Wang Z, Xiao W, Liu W, Wang X (2018) Endoplasmic reticulum stress in the heart insights into mechanisms and drug targets. Br. J. Pharmacol 175:1293–1304

Weintraub AS, Li CH, Zamudio AV, Sigova AA, Hannett NM, Day DS, Abraham BJ, Cohen MA, Nabet B, Buckley DL, Guo YE, Hnisz D, Jaenisch R, Bradner JE, Gray NS, Young RA (2017) YY1 is a structural regulator of enhancer promoter loops. Cell 171:1573–1588.e28

Williams RS (1999) Apoptosis and heart failure. NEJM 341:759–760

Xiao R, Chen JY, Liang Z, Luo D, Chen G, Lu ZJ, Chen Y, Zhou B, Li H, Du X, Yang Y, San M, Wei X, Liu W, Lécuyer E, Graveley BR, Yeo GW, Burge CB, Zhang MQ et al (2019) Pervasive chromatin-RNA binding protein interactions enable RNA-based regulation of transcription. Cell 178:107–121.e18

Xing F, Zhan Q, He Y, Cui J, He S, Wang G (2016) 1800 MHz microwave induces p53 and p53-mediated caspase-3 activation leading to cell apoptosis in vitro. PloS one 11:e0163935

Yang Y, Liu L, Naik I, Braunstein Z, Zhong J, Ren B (2017) Transcription factor C EBP homologous protein in health and diseases. Front. immunol 8:1612

Yao Y, Lu Q, Hu Z, Yu Y, Chen Q, Wang QK (2017) A non canonical pathway regulates ER stress signaling and blocks ER stress induced apoptosis and heart failure. Nat Commun 8:133

Yu H, Chen B, Ren Q (2019) Baicalin relieves hypoxia-aroused H9c2 cell apoptosis by activating Nrf2 HO-1-mediated HIF1α BNIP3 pathway. Artif Cells Nanomed Biotechnol 47:3657–3663

Yuan M, Gong M, Zhang Z, Meng L, Tse G, Zhao Y, Bao Q, Zhang Y, Yuan M, Liu X, Li G, Liu T (2020) Hyperglycemia induces endoplasmic reticulum stress in atrial cardiomyocytes and mitofusin 2 downregulation prevents mitochondrial dysfunction and subsequent cell death. Oxid. Med. Cell. Longev. OXID MED CELL LONGEV 2020:6569728

Zhou A, Ou AC, Cho A, Benz EJ Jr, Huang SC (2008) Novel splicing factor RBM25 modulates Bcl x pre mRNA 5' splice site selection. Mol. Cell. Biol 28:5924–5936

Publisher's Note Springer Nature remains neutral with regard to jurisdictional claims in published maps and institutional affiliations.

Springer Nature or its licensor (e.g. a society or other partner) holds exclusive rights to this article under a publishing agreement with the author(s) or other rightsholder(s); author self-archiving of the accepted manuscript version of this article is solely governed by the terms of such publishing agreement and applicable law.